Biochimie 182 (2021) 51–60

Contents lists available at ScienceDirect

Biochimie

journal homepage: www.elsevier.com/locate/biochi

Purification and characterization of a novel and conserved TPR-domain protein that binds both Hsp90 and Hsp70 and is expressed in all developmental stages of *Leishmania major*

Sara A. Araujo [a], Gustavo H. Martins [a], Natália G. Quel [a, b], Annelize Z.B. Aragão [a], Edna G.O. Morea [c], Julio C. Borges [b, d], Walid A. Houry [e, f], Maria I.N. Cano [c], Carlos H.I. Ramos [a, b, *]

[a] Institute of Chemistry, University of Campinas UNICAMP, Campinas, SP, 13083-970 Brazil
[b] National Institute of Science & Technology of Structural Biology and Bioimage (INCTBEB), Brazil
[c] Department of Chemical and Biological Sciences, Biosciences Institute, Sao Paulo State University, Botucatu, SP, 18618689, Brazil
[d] São Carlos Institute of Chemistry, University of São Paulo, São Carlos, SP, Brazil
[e] Department of Biochemistry, University of Toronto, Toronto, Ontario, M5G 1M1, Canada
[f] Department of Chemistry, University of Toronto, Toronto, Ontario, M5S 3H6, Canada

ARTICLE INFO

Article history:
Received 30 August 2020
Received in revised form
14 December 2020
Accepted 26 December 2020
Available online 6 January 2021

Keywords:
TPR-Domain protein
Leishmania major
Hsp90 co-chaperones
Protein folding
Protein structure and function

ABSTRACT

Heat shock proteins (Hsps) are involved in several important aspects of the cell proteostasis. Hsp90 interacts with at least a tenth of the cell proteome helping a large number of proteins to fold correctly. Hsp90 function is modulated by several co-chaperones having TPR (tetratricopeptide repeat) domains that allow for interaction with the C-terminal MEEVD motif of the chaperone. Another important chaperone, Hsp70, has a C-terminal EEVD motif that binds to TPR. *Leishmania* is a protozoan that causes leishmaniasis, a neglected disease in humans and other animals. There is still no effective treatment for leishmaniasis, however the study of structure and function of the proteins of the parasite may generate potential targets for future therapeutic intervention studies. In this work, the genome of *Leishmania major* was searched for a novel TPR-domain gene, which is conserved in Leishmania. The recombinant protein, LmTPR, was produced in pure and folded state and was characterized by biophysical tools as a monomer with an elongated conformation. Studies in *Leishmania major* were also preformed to complement these *in vitro* experiments. Splice Leader RNA-seq analysis and Western blot indicated that the protein was expressed in all developmental stages of the parasite. Binding assays confirmed that both Hsp90 and Hsp70 bind specifically to LmTPR. Finally, sequence and structural predictions indicated a C-terminal region as a RPAP3 domain. Altogether, this study identified a novel TPR-domain co-chaperone of Hsp90 that is conserved and expressed in all developmental stages of *Leishmania major*.

© 2021 Elsevier B.V. and Société Française de Biochimie et Biologie Moléculaire (SFBBM). All rights reserved.

1. Introduction

A cell proteome is much more than the expressed proteins coded in its genome because proteins expand their functions via a network of interactions with other molecules, mainly proteins. The 90 kDa heat shock protein (Hsp90) is one of the principal components of the machinery that maintains proteostasis in the cell and interacts with at least 10% of the proteome [1–3]. Many of these interactions are with co-chaperones that modulate the conformational changes of Hsp90 and therefore its function [3,4]. A large portion of the co-chaperones interact with Hsp90 via a TPR domain [3–5]. TPR, tetratricopeptide repeat region, contains a minimum of 34 amino acid residues arranged in a helix-turn-helix fashion, and adjacent TPR motifs can pack in a spiral way creating a groove with a large surface area for binding ([6]; see also Fig. 1). The C-termini motifs of cytoplasmic Hsp90 (MEEVD) and Hsp70 (EEVD) have a

Abbreviations: CD, circular dichroism; Hsp, heat shock protein; SEC-MALS, size exclusion chromatography coupled to multi-angle light scattering.

* Corresponding author. Institute of Chemistry, University of Campinas UNICAMP, Campinas, SP, 13083-970 Brazil.
E-mail address: cramos@unicamp.br (C.H.I. Ramos).

https://doi.org/10.1016/j.biochi.2020.12.017
0300-9084/© 2021 Elsevier B.V. and Société Française de Biochimie et Biologie Moléculaire (SFBBM). All rights reserved.

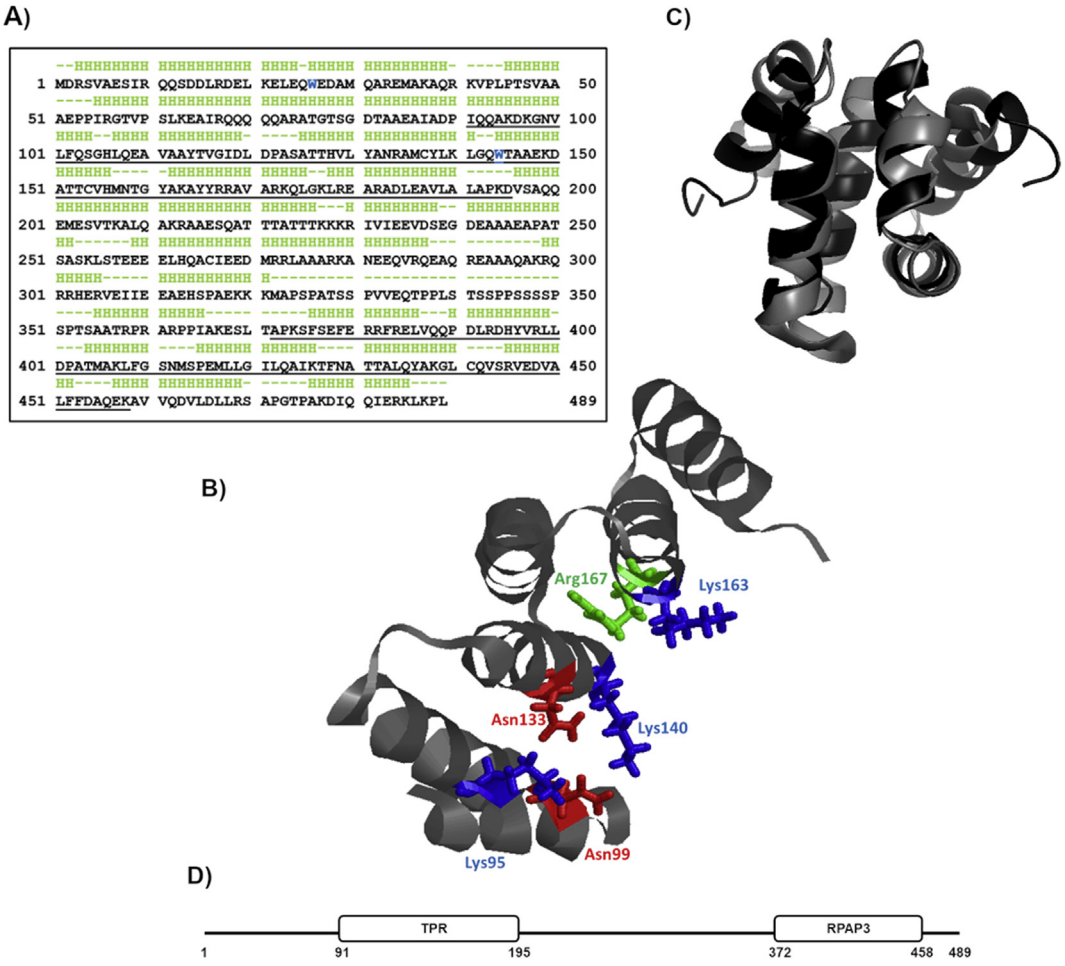

Fig. 1. A) Amino acid sequence. The amino acid sequence of the putative TPR-domain protein from *Leishmania major* (NCBI accession XP_003722051). Protein is 489 amino acid long and predicted helices, as analyzed by PSIPRED and Jpred, are indicated (H). Prosite analysis found two TPR repeats from 91 to 124 and 162–195 forming a TPR-region (91–195). Pfam analysis found three TPR repeats in the sequence: 98–128 (e-value 4e-4), 130–153 (e-value 2.9e-5) and 162–195 (e-value 8.9e-3), and also a potential Monad-binding region of RPAP3 from residues 372 to 458 (e-value 7.6e-14). Interpro 79.0 (EMBL) analysis found a TPR domain from residues 91 to 195 and an RPAP3 domain from residues 372 to 458 (both sequences are underlined). From the sequence, the molecular mass is of about 53.6 kDa and pI is predicted as 6.5. Trp residues are in positions 26 and 144 (W, blue). **B) TPR-domain**. *Ab initio* structure prediction of region 91–195 was performed using Quark online software (see Material and Methods). Three tetratricopeptide repeat regions, each arranged in a helix-turn-helix fashion, are packed in a spiral way. Residues (K95, N99, N133, K140, K163 and R167) involved with MEEVD motif binding are shown. **C) Structure alignment.** The structure prediction for residues 372–458 from LmTPR (gray) is highly similar (RMS of 2.45 Å) to the NMR structure of the C-terminal domain of human RPAP3 protein (PDB 6EZ4; black). See also Supplementary Video 1. **D) Domain arrangement.** Cartoon of LmTPR domain arrangement.

large affinity for this surface [7]. Examples of Hsp90 co-chaperones with TPR-domain are CHIP (carboxy terminus of Hsp70 binding protein), HOP (Hsp70/Hsp90 organizing protein), Tah1 (TPR- containing protein associated with Hsp90), and others.

The relevance of studying proteins from *Leishmania* lies in the fact that this trypanosomatid causes leishmaniasis in humans and animals and against which there is no effective treatment [8]. Therefore, the study of structure and function of its proteins may generate potential targets for future therapeutic interventions. A search of the genome of *Leishmania major* revealed a putative TPR-repeat protein (NCBI accession XP_003722051), referred to here as LmTPR protein. SL-RNA seq analysis confirmed that the gene was expressed in all developmental stages of *Leishmania major*. DNA sequence was used to generate a clone inserted into a pET vector to produce the recombinant protein. Recombinant LmTPR protein was purified in its folded state as a monomer and was able to interact with both Hsp90 and Hsp70. Importantly, specific immune serum produced against the recombinant LmTPR protein recognized a protein expressed in all developmental stages of the parasite, supporting the SL- RNA-seq analyses. Moreover, the protein is conserved in other Leishmania species suggesting that it is important to modulate the functions of Hsp90 and Hsp70 and thus have the potential to be considered a target for intervention in future studies.

2. Material and methods

2.1. Sequence analysis

Sequence analysis was done by PSIPRED [9], Jpred4 [10], InterPro [11], Pfam [12], and Prosite [13] and sequence alignment by Clustal Omega [14]. Blast [15] was used to search the gene in Leishmania, to generate a distance tree based on alignment similarity scores and to perform multiple alignments. *Ab initio* structure prediction was performed using Quark online software [16,17].

2.2. Protein expression and purification

The putative TPR-repeat protein from *Leishmania major* (NCBI accession XP_003722051; gene ID LmjF.27.2390) coding sequence

was optimized for expression in *Escherichia coli* and cloned into a pET28a vector between *Bam*HI and *Xho*I sites (Epoch LifeSciences Inc. custom cloning) for the creation of a His-tag at the N-terminus. The expression of LmTPR protein was carried out using BL21 (DE3) ArcticExpress® (Agilent Technologies). Cells were grown overnight at 37 °C in LB medium containing 100 μg mL^{-1} kanamycin and 200 μg mL^{-1} gentamicin under constant shaking at 200 rpm (Forma Orbital Shaker – Thermo Scientific). After 16 h, 10 mL of culture was added to 500 mL LB medium, and cells were allowed to grow at 30 °C until the absorbance (A_{600}) reached 0.6–0.8 (Spectrophotometer SP1102 – Tecnal). Protein expression was induced at 12 °C by adding 1.0 mM isopropyl thio-β-Dgalactoside (IPTG). After 24 h, cells were harvested by centrifugation at 2496 g for 15 min at 4 °C and the pellet resuspended in 45 mL of buffer containing 25 mM Tris-HCl, pH 8.0, 150 mM NaCl (Buffer A), 30 μg mL^{-1} Lysozyme, 1.0 mM PMSF and 5 U DNase. After incubation for 30 min on ice, sonication was performed in an ultrasonic processor (Misonix) with an amplitude of 30 Watts, pulsing 5 s with an interval of 1 min, within 2 min of total process time. The cell lysate was centrifuged at 4 °C, for 15 min at 12000 g (Allegra Beckman-Coulter) and the supernatant was filtered through a 0.45 μm membrane (Millipore). Protein was purified by two chromatographic steps: the first was Ni^{2+} affinity chromatography using a 5 mL HisTrap HP column (GE Healthcare, NJ, USA) equilibrated with Buffer A and eluted in the same buffer containing 500 mM Imidazole-Cl using a peristaltic pump. The second step was size exclusion chromatography using a Superdex 200 Hiload 26/60 column (GE Healthcare, NJ, USA) previously equilibrated in Buffer A, coupled to an ÄKTA Pure (GE Healthcare, NJ, USA). Protein purity was assessed by combining SDS-PAGE (10%) and ImageJ [18] analyses. Protein concentration was measured by spectroscopy according to the Edelhoch method [19]. Rabbit polyclonal antibodies were produced (Rhea Biotech Ltda) using the recombinant LmTPR protein and these antibodies were used to explore *Leishmania* extracts in western blot experiments (see below). Hsp90 from *L. braziliensis* and human Hsc70 (Hsp70.1) were purified as previously described ([20,21] respectively).

2.3. Western blot and SL-Seq analyses

Leishmania major strain (MHOM/IL/1980/FRIEDLIN) was a genetically homogenous population from the Oswaldo Cruz Institute collection. For precaution, parasite cultures were screening against Mycoplasma using the MycoFluor™ Mycoplasma Detection Kit (Molecular Probes) and no contamination was detected. Parasite life stages were originated from the same developmental cycle, i.e. amastigotes extracted from mice footpad lesions [22] were differentiated *in vitro* into newly transformed promastigotes. Promastigote forms were cultivated in an exponential phase at 26 °C in 1X M199 medium, pH 7.3, supplemented with 10% (v/v) heat-inactivated fetal calf serum, 25 mM HEPES and 1% (v/v) antibiotic/antimycotic solution (all reagents from Cultilab), and the metacyclic stage was selected from stationary phase promastigotes cultures using agglutination with peanut lectin [23]. After that, parasite cells (~2×10^8 total) were washed twice with 1X PBS, resuspend in 1 mL of buffer A (20 mM Tris-HCl, pH 7,5, 1 mM EGTA, 1 mM EDTA, 15 mM NaCl, 1 mM spermidine, 0.3 mM spermine, and 1 mM DTT), frozen in liquid nitrogen for 1 min and then thawed on ice. This sample was incubated with 0.5% Nonidet p-40 on ice for 30 min, centrifuged at 8000×*g* to discard the pellet, and 1X of protease inhibitor cocktail (Sigma) was added. Approximately 10% of this protein extract (corresponding to 2×10^7 cells or approximatelly 100 μg total protein per lane) were fractionated onto 12% SDS-PAGE and transferred to nitrocellulose membranes (BioRad). Western blots were then developed using a goat anti-rabbit HRP-conjugated secondary antibody (Bio-Rad) and the enhanced chemiluminescence (ECL), according to the manufacturer's instructions (Millipore). Anti-LaRbp38 and anti-LmGAPDH were used as loading controls.

Independent SL-RNA-Seq libraries (one biological replicates each) from *L. major* life stages (amastigote, promastigote, and metacyclic) were constructed by Peter Myler's laboratory, as previously reported [24] and their good quality verified by FastQC (https://www.bioinformatics.babraham.ac.uk/projects/fastqc/). Worthy mentioning, libraries were provided by Peter Myler's Laboratory to the TriTrypDB web resource (https://tritrypdb.org/tritrypdb/app/record/dataset/DS_8bc463a882) and used to map the 5′UTR of *L. major* Friedlin genes in the TritrypDB. The libraries were then aligned against *L. major* Friedlin genome (TriTyrpDB v38*) with bowtie2 (PMID: 22388286) [25], using the following parameters: –very-sensitive-local -N 1. Bowtie2-generated bam files were loaded into the Artemis genome browser (PMID: 22199388) [26] to compute RPKM (Reads Per Kilobase of the transcript, per Million of mapped reads) values [27] using as a parameter an arbitrary length of 250 nt surrounding the left- or right-most non-CDS SL signal positioned 5′ upstream of each gene analyzed (TPR, LmjF.27.2390; RBP38, LmjF.23.0760; and GAPDH, LmjF .30.2970 and .30.2980).

2.4. Spectroscopy

Circular dichroism (CD) measurements were performed on a Jasco J-720 spectropolarimeter coupled to a PFD 425-S (Jasco) Peltier - type control system using standard parameters [28]. Data were collected from 260 to 200 nm, at 25 °C, with a bandwidth of 1.0 nm and a response time of 4 s, data were averaged at least four times. All measurements were made in a quartz cuvette with 2 mm optical path length with 2.0 μM protein in Buffer A. Buffer measurements were subtracted and measurements were normalized to the mean residual molar ellipticity ([θ]). Thermal-induced unfolding was performed from 20 to 90 °C, while urea-induced unfolding was performed from 0 to 8 M urea at 20 °C. Induced unfolding assays used 1.5 μM of LmTPR protein in Buffer A, CD signal at 222 nm, with a bandwidth of 1.0 nm and a response time of 4 s in cuvettes with a 5 mm optical pathlength.

Intrinsic fluorescence emission measurements were recorded in an Aminco Bowman® Series 2 – Luminescence Spectrometer using a quartz cuvette with a 10 mm optical pathlength at 20 °C. Protein concentration was 10.0 μM in Buffer A with or without the presence of 8 M urea. The emission fluorescence spectra of tryptophan were obtained with excitation at 295 nm and emission from 300 to 400 nm.

2.5. Hydrodynamic parameters

For details and equations see Ref. [29]. Dynamic light scattering (DLS) experiments were performed on a Zetasizer NANO ZEN 3600 (Malvern) at 25 °C with protein concentration from 10 to 80 μM in Buffer A to measure the translational diffusion coefficient (D). Analytical size exclusion chromatography experiments were carried out using a Superdex 200 10/300 GL column (GE Healthcare), coupled to an ÄKTA FPLC device (GE Healthcare) equilibrated with Buffer A. LmTPR protein at a concentration of 40 μM was loaded onto the column at a flow rate of 0.5 mL min^{-1} and the elution profile was monitored by absorbance at 280 nm. The column was previously calibrated with a mix of standard proteins with known Stokes radius (R_s): Aldolase (48.1 Å); Conalbumin (36.4 Å); Ferritin (61.0 Å); Ovalbumin (30.5 Å); Thyroglobulin (85.0 Å) (GE Healthcare). All standard proteins were prepared in concentration 2 mg mL^{-1} in Buffer A. The R_s of each standard protein was plotted

against -(log Kav)^{½} (Kav = (Ve - Vo)/(Vc - Vo)) and adjusted by linear fitting analysis. The fitting parameter was applied to calculate the R_S for LmTPR protein. Size exclusion chromatography coupled to a multiple-angle light scattering (SEC-MALS) experiments were performed at 20 °C using a triple-angle static light scattering detector (miniDAWN™ TREOS) and a refractive index monitor (Optilab® T-rEX) (Wyatt Technology) coupled to an ÄKTA FPLC system, with UV/Vis detector (GE Healthcare). LmTPR protein at a concentration of 4 μM was injected onto a Superdex 200 10/300 GL (GE Healthcare) and eluted in Buffer A. Then, data were processed using the ASTRA 6.0 software (Wyatt Technology) to obtain the protein molecular mass.

2.6. Interaction with LbHsp90 and HsHsc70

Interaction experiments were performed using the available *Leishmania braziliensis* Hsp90 recombinant protein, which is >97% identical to *Leishmania major* Hsp90 [20] and/or human Hsc70, wich is >72% identical to *L. major*. Experiments were performed by mixing 19 μM of dimeric Hsp90 with 38 μM of LmTPR (1:2 dimer to monomer concentration, respectively) or 15 μM of Hsc70 with 15 μM of LmTPR (1:1 monomer to monomer) in Buffer A. The LbHsp90 and LmTPR mixture was incubated at 4 °C for 150 min, under constant and gentle agitation while Hsc70 and its mixture with LmTPR were overnight dyalized to the Buffer A. The mixtures, isolated proteins and controls were subsequently subjected to SEC-MALS (Optilab T-rEX and miniDAWN TREOS instruments,Wyatt Technology) by applying 500 μL to a Superdex 200 Increase 10/300 GL (ÄKTA FPLC). Data were analyzed using the Astra 6 software. The column was previously equilibrated with the same buffer and the runs were performed at 0.5 mL min^{-1}. As negative controls, chaperones were mixed with BSA (ThermoFisher Scientific) and analyzed under the same conditions. Fractions corresponding to the free proteins, as well as the mixtures, were collected and compared by SDS-PAGE, followed by quantitative analysis using the ImageJ software as described above.

3. Results and discussion

3.1. LmTPR was produced pure and expressed in all developmental stages of Leishmania major

From its sequence (Fig. 1A), the putative TPR-domain protein (NCBI accession XP_003722051) is 489 amino acids long with a molecular mass of about 53.6 kDa (His-tag added 17 residues resulting in a molecular mass of 55.5 kDa, and a theoretical isoelectric point of about 7). Secondary structure prediction suggests an alpha-helical protein (Fig. 1A), a result supported by circular dichroism measurements (see below). The region from residues 91–195 (underlined in Fig. 1A) was considered a TPR-domain by three different predictors and has the proper conformational arrangement that characterizes such domain, as supported by *ab initio* protein structure prediction (Fig. 1B). Also shown, are residues (K95, N99, N133, K140, K163 and R167) involved with MEEVD motif binding, which are conserved among several species (as, for instance, yeast, Drosophila, Arabidopsis and human; data not shown) (Fig. 1B). The side chains of these residues are at the groove of the TPR-domain, which have a large surface area for effective binding to MEEVD (Fig. 1B). Two of the predictors also suggest the presence of a potential RPAP3 domain found at the C-terminus of RNA-polymerase II-associated proteins (underlined in Fig. 1A), which was also supported by *ab initio* protein structure prediction (Fig. 1C). As a matter of fact, the structure prediction os this region in LmTPR, residues 372–458, indicated a high similarity (RMS of 2.45 Å) to the NMR structure of the C-terminal domain of human RPAP3 protein (PDB 6EZ4) (Fig. 1C). Finally, Fig. 1D shows the proposed domain arrangement of LmTPR.

The recombinant protein was produced with a His-tag at its N-terminus for purification purposes, increasing its molecular mass to of about 55.5 kDa (Fig. 2), and was purified by two chromatographic steps. The first step was His-tag affinity chromatography and generated a protein with a high degree of purity (Fig. 2A) and the second step was size exclusion chromatography that showed a major peak (Fig. 2B and C) corresponding to a monomeric species (see below). At the final process, the purity of the LmTPR protein was higher than 95%.

Once it was confirmed that the DNA sequence was translated into a stable protein, it was necessary to identify whether or not it was expressed by *L. major* cells. First, independent Splice Leader (SL) RNA-Seq (SL-RNA-Seq) libraries analyses showed that LmTPR was expressed in the three parasite developmental stages (amastigotes, procyclic promastigotes, and metacyclics) (Fig. 3, top). Noteworthy, as in other trypanosomatids, in *Leishmania* sp. mRNAs are processed by *trans*-splicing, i.e. the addition of a SL (splice

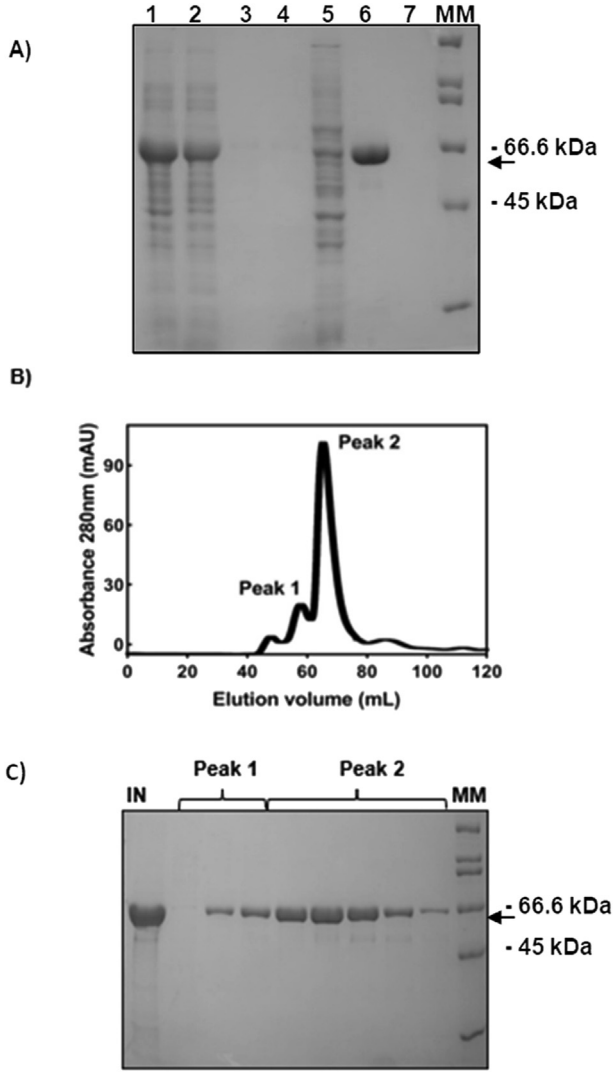

Fig. 2. Protein purification. A) Ni^{+2} affinity chromatography analyzed by SDS-PAGE (10%). Samples: bacterial lysate soluble fraction: 1; flow-through: 2–4; buffer wash; imidazole wash: 5 (40 mM), 6–7 (500 mM). **B) SEC** followed by **C) SDS-PAGE (10%).** Peak 2 has most of the purified protein with more than 95% purity. MM: molecular mass standard; bands corresponding to 66.2 and 45.0 kDa are indicated. Purification yield was 13 g L^{-1} of culture. Arrow, LmTPR protein.

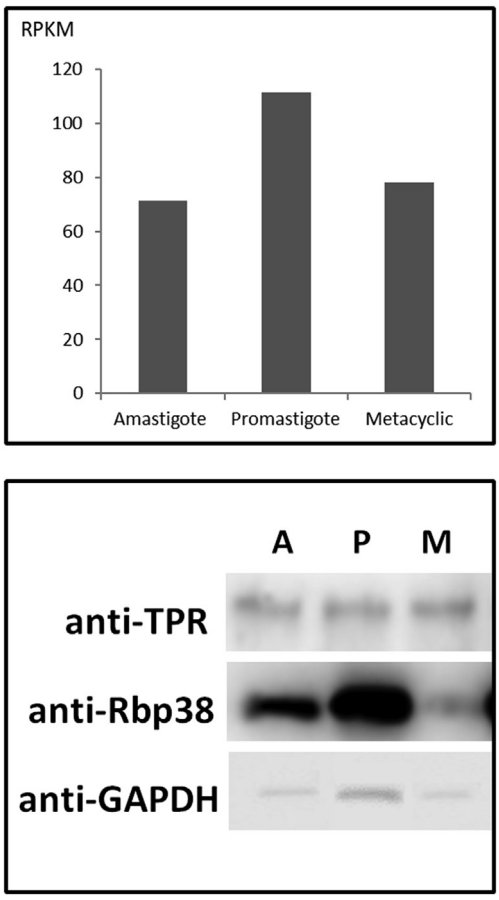

Fig. 3. Top. RPKM calculated from the LmTPR gene of all three *Leishmania major* life stages. Amastigote, promastigote, and metacyclic stages are indicated. Additional information is available in Supplementary Table 1. **Bottom. LmTPR is expressed in all *L. major* developmental stages.** Western blot analysis was done with total protein extracts obtained from approximately 2×10^7 *L. major* cells using a specific polyclonal antibody that recognizes LmTPR (see Material and Methods). Loading controls are anti-LaRbp38 and anti-LmGAPDH. Stages are amastigote (A), promastigote (P), and metacyclic (M).

leader) sequence (a tri-methyl guanosine 5′capped wich is 39 nt long) is coupled with the addition of a poly-A tail at the 3′ end of the upstream gene in the polycistron [30]. Therefore, SL is a conserved marker of RNA maturation in trypanosomatids and the SL-RNA-seq libraries are sequenced based on the presence of the SL sequence at the 5′ end of each transcript [23]. Two biological replicates of each library were analyzed and the RPKM (Fig. 3-top; Table S1) represents the average obtained from them. The difference in mRNA levels between promastigotes and amastigotes and metacyclics is probably due to unknown regulatory elements at the LmTPR 3′UTR [31–33]. In this case, regulatory elements would positively control mRNA expression and stabilization only in promastigotes, justifying the results obtained in the SL-seq libraries. Accordingly, genetic reprogramming, during parasite development induces differences in promastigotes and even up amastigotes and metacyclics in respect of gene expression profiles [34] and differences in mRNA abundance during parasite development were widely described for *Leishmania* sp [35–37].

Additionally, polyclonal antibodies were produced using the recombinant protein (see Supplementary Figure S1) and were used to explore extracts from *Leishmania major* in western blot experiments (Fig. 3, bottom) using anti-LmRbp38 and anti-LmGAPDH as loading controls. The analysis of Fig. 3 clearly shows the identification of a protein with a mass similar to that of LmTPR in all developmental stages of the parasite, and few differences in protein abundance among parasite life stages, compared to the proteins used as the loading controls. In this context, it is important to point that the regulation of both mRNA and protein levels dynamically alters in Leishmania because they depend on both the function of parasite adaptation to new environmental circumstances and the host [38].

Since results indicated that the protein is expressed in *Leishmania major* cells, Blast was used to investigate whether or not the protein was present in other *Leishmania* species. Fig. S2A shows that homologues of LmTPR are present in all *Leishmania* species analyzed (*Leishmania donovani*, *Leishmania infantum*, *Leishmania mexicana*, *Leishmania tarentolae*, *Leishmania guyanensis*, *Leishmania panamensis* and *Leishmania braziliense*s) and is highly conserved. A distance tree based on alignment similarity scores (Fig. S2B) and multiple sequence alignments (Fig. S2C) are also shown. Altogether these results indicate that LmTPR is conserved within the *Leishmania* genus, a feature that supports the hypothesis that the protein is important to interact (see below) and aid Hsp90 with its functions.

3.2. LmTPR was produced folded as an elongated monomer

LmTPR protein was produced folded as verified by circular dichroism (CD) and fluorescence spectroscopies (Fig. 4). The CD spectrum (Fig. 4A) shows two negative bands of different intensities at about 222 and 208 nm, a profile characteristic of α-helical proteins, and the helical content was estimated to be about 27%. However, the much lower signal at 208 nm than at 222 nm could indicate that some portion of the protein may have random secondary structure.

LmTPR protein has two Trp residues (see Fig. 1) and the analysis of their emitted fluorescence (Fig. 4B), which is sensitive to polarity, helps to understand the environment they experience in the purified protein because a well-buried Trp residue emits at wavelengths lower than 330 nm, while a completely exposed Trp residue emits at wavelengths greater than 350 nm (for review see Ref. [39]). The wide shape spectrum displayed in Fig. 4B at native conditions is indicative that the two Trp residues had distinct maximum wavelength, one of about 335 nm and the other of about 355 nm. When the protein was unfolded by 8 M urea, only one maximum was identified of about 355 nm (Fig. 4B). The most likely explanation is that, at native conditions, one of the two Trp residues was well-buried in the protein while the other was more exposed to the solvent and both become exposed when the protein was unfolded (Fig. 4B). Since one of the Trp residues, W144 (Fig. 1), is located in the predicted well-folded TPR domain, we suggest that the exposed Trp is W26 (Fig. 1). In support of this hypothesis, the *ab initio* structure predicted that the W144 is well buried in the structure (Fig. 4B, inset).

The stability of the protein was investigated by both thermal- (Fig. 4C) and urea-induced unfolding followed by CD at 222 nm (Fig. 4D). The thermal-induced unfolding analysis of Leishmania proteins is important because the parasite lives in organisms with different body temperatures. During the parasite developmental cycle, flagellated promastigote and metacyclic forms living in the invertebrate host (sandflies, 28 °C) transform into nonflagellated and intracellular amastigotes infecting a mammalian host (e.g. humans, 37 °C [40]. Little change in secondary structure, of about 10%, was detected up to 37 °C, the human body temperature. However, raising the temperature above this point resulted in the unfolding of the protein at about 70 °C, which was irreversible but folding reversibility was reached when the protein was heated only up to 55 °C (data not shown). The non-two-state profile of the

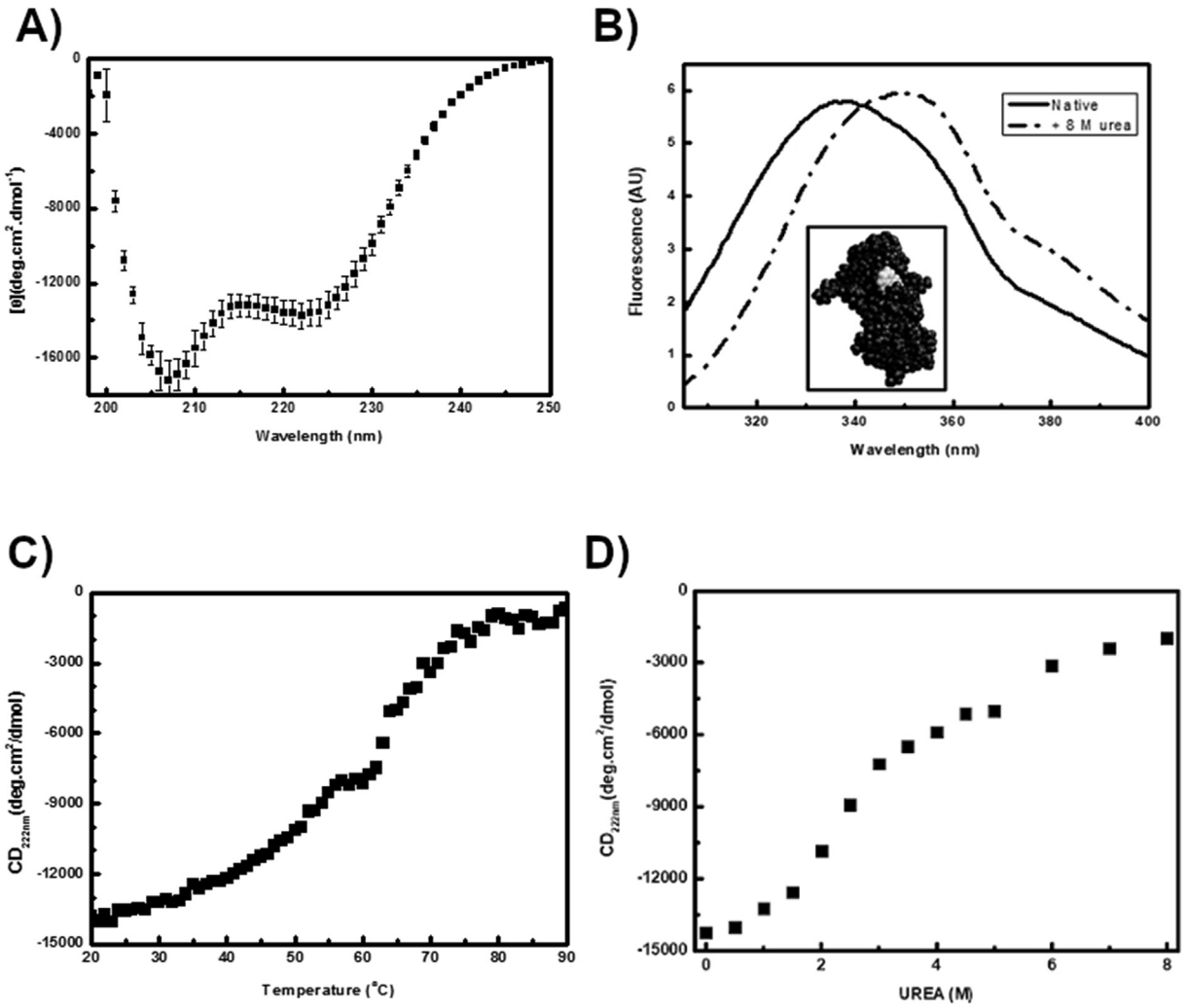

Fig. 4. Spectroscopic analysis. A) Circular dichroism. CD was measured from 260 to 200 nm at 25 °C and acquired in the buffer A (25 mM Tris-HCl (pH 8.0) containing 150 mM NaCl), the data was normalized for mean molar residual ellipticity ([θ]). The spectrum is characteristic of an α-helix conformation with minima signals at 208 and 222 nm and positive at about 200 nm. **B) Fluorescence.** The intrinsic (Trp residues) fluorescence emission spectrum was obtained with exciting the sample at 295 nm and data collected from 300 to 400 nm in Buffer A at 20 °C both in the presence and in the absence of 8 M urea. The wide shape spectrum at native conditions is an indication that the two Trp residues had distinct maxima wavelength, one of about 335 nm and the other of about 355 nm. When the protein was unfolded by 8 M urea, only one maximum was identified of about 355 nm. Inset: All-atom predicted conformation of the folded TPR-domain highlighting the Trp position, which is well-buried. **C) Temperature-induced unfolding.** Thermostability was investigated by temperature-induced unfolding followed by CD at 222 nm and complete unfolding was at about 70 °C, which was irreversible. Folding reversibility was reached when the protein was heated only up to 55 °C. **D) Urea-induced unfolding.** Urea-induced unfolding was performed from 0 to 8 M urea at 20 °C and followed by CD at 222 nm.

unfolding curve (Fig. 4C) indicated that the protein apparently has at least two domains with different stabilities, a result supported by the urea-induced unfolding results (Fig. 4D) and sequence analysis (Fig. 1). Altogether, these results suggest that the protein likely has multiple domains with different stabilities but in general is stable at the temperatures experienced by the parasite in its life cycle.

The hydrodynamic parameters were investigated by analytical SEC, DLS, and SEC-MALS. Analytical SEC investigation showed that the protein had a Stokes or hydrodynamic radius, R_s, of 51 ± 1 Å (Fig. 5A). DLS investigation showed that the protein had a diffusion coefficient, D, of 3.4 ± 0.2 × 10^{-7} cm^2 s^{-1} (Fig. 5B). SEC-MALS investigation showed that the protein had a molecular mass, MM, of 57 ± 1 kDa (Fig. 5C), a value analogous to that of a monomer. To get information about the conformation of the protein, we calculated the values of R_s and D for a non-hydrated sphere with the same MM of a LmTPR monomer and compared it to those measured for LmTPR protein (Table 1). The measured values are very different from that predicted, indicating that the protein is nonglobular and likely has an elongated shape. Worth mentioning, TPR co-chaperones of Hsp90 from several organisms usually have an elongated conformation [41–43].

3.3. LmTPR interacts with both Hsp90 and Hsp70

The Hsp90 family is one of the main hub proteins in the cell. It interacts with about 10% of the proteome in yeast and together with Hsp70 forms a subsystem involved in maintaining proteostasis [1–3]. Proteins of a wide variety of functions are clients of Hsp90 and/or Hsp70 to reach their mature state. The interaction with different co-chaperones is crucial for Hsp90 and Hsp70 to interact and aid the folding of its plethora of clients. A large number of proteins that interact with Hsp90/Hsp70 have a TPR-domain to interact with the C-terminal MEEVD/EEVD motifs of the chaperones, thus justifying the search and characterization of such protein in different organisms. The validation of LmTPR protein as an interactor of Hsp90/Hsp70, was done by using SEC to investigate

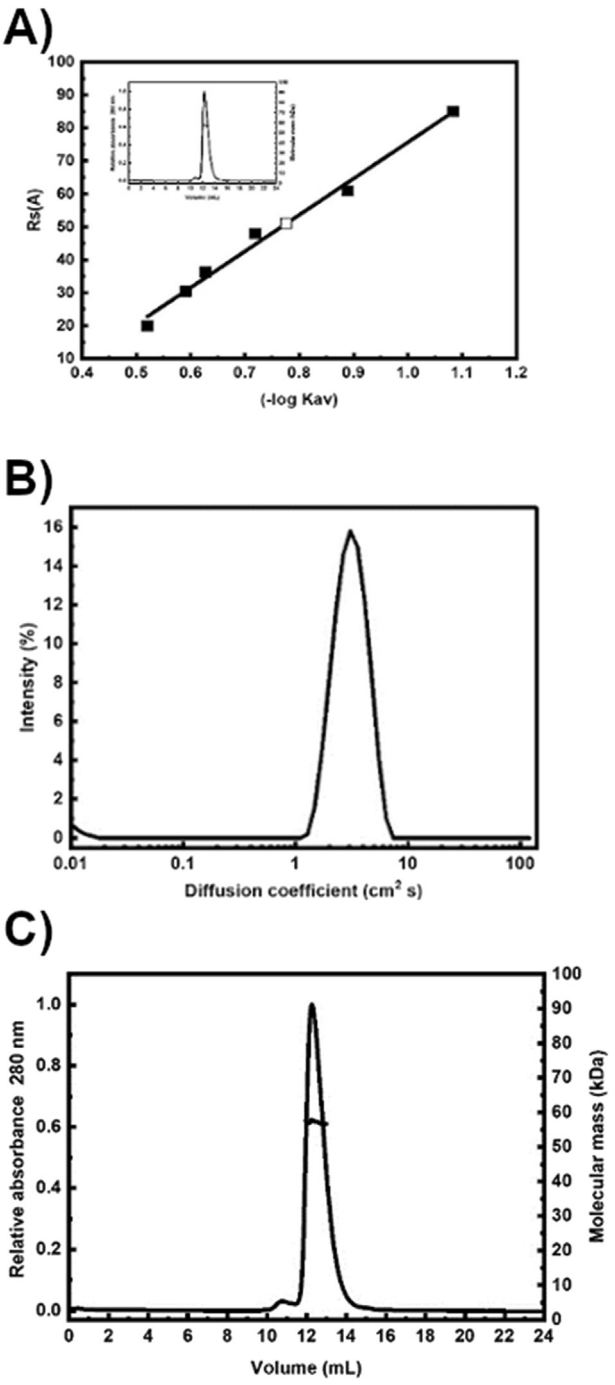

Fig. 5. Hydrodynamic investigation. A) Analytical SEC experiment was performed in buffer A and R_s (Stokes or hydrodynamic radius) was about 51 Å. **B**) DLS investigation showed a diffusion coefficient, D, of $3.4 \pm 0.2 \times 10^{-7}$ cm^2 s^{-1}. **C**) SEC-MALS was performed to determine the absolute molecular mass in solution, which was 57 ± 1 kDa and analogous to that of a monomer.

Table 1
Hydrodynamic parameters.

Parameter	Measured	Predicted[a]
D (10^{-7} cm^2 s^{-1})	3.4 ± 0.2	9
R_s (Å)	51 ± 1	25

[a] For a non-hydrated sphere with the same MM of monomeric LmTPR protein.

whether or not these proteins bind to each other by co-eluting.

SEC experiment (Fig. 6A) shows that isolated LbHsp90 and LmTPR elute at different volumes as they have different molecular masses. LbHsp90 is a dimer with about 182 kDa (eluted mainly at 11 and 12 mL, as shown in Fig. 6A) and LmTPR protein is a monomer with about 55.5 kDa (eluted mainly at 12 and 13 mL, Fig. 6A). Interestingly, when mixed, a portion of the proteins interact and elute as higher molecular mass species (mainly 10 and 11 mL, Fig. 6A) than the isolated proteins. ImageJ analysis helped again in this evaluation (data not shown). According to it, LbHsp90 alone eluted mainly at fractions (in mL) 10 (11 ± 1%), 11 (40 ± 2%), 12 (30 ± 1%) and 13 (11 ± 1%) and LmTPR alone eluted mainly at volumes 12 (41 ± 2%), 13 (33 ± 2%) and 14 (12 ± 1%). However, the pattern was different when the proteins were loaded together: LbHsp90 eluted mainly at volumes 10 (29 ± 3%), 11 (40 ± 1%) and 12 (18 ± 3%) and LmTPR alone elutes mainly at volumes 10 (12 ± 3%), 11 (28 ± 3%), 12 (38 ± 1%) and 13 (15 ± 1%). Summing up, in volumes 10 mL plus 11 mL, which represent a higher molecular mass than the isolated proteins, the participation of Hsp90 increased from 52 ± 1 to 69 ± 2% and LmTPR from 0 to 41 ± 1%. For raw data see Supplementary Table S2. Additionaly, the mixture fraction was submitted to SEC-MALS that indicated a molecular mass of 248 ± 10 kDA, very similar to the predicted of 230 kDa.

Another SEC experiment was used to evaluate the interaction between human Hsc70, since Leishmania Hsp70 is insoluble [44], and LmTPR. HsHsc70 is a monomer with about 70.8 kDa (eluted mainly at 14 and 15 mL, as shown in Fig. 6B) and LmTPR protein is a monomer with about 55.5 kDa (eluted mainly at 13 and 14 mL, Fig. 6B). Interestingly, when mixed, a portion of the proteins interact and elute as higher molecular mass species (mainly 11 and 12 mL, Fig. 6B) than the isolated proteins. ImageJ analysis helped again in this evaluation (data not shown). According to it, Hsc70 alone eluted mainly at fractions (in mL) 12 (4 ± 1%), 13 (14 ± 1%), 14 (29 ± 1%) and 15 (42 ± 2%) and LmTPR alone eluted mainly at volumes 11 (10 ± 1%), 12 (17 ± 1%), 13 (42 ± 2%) and 14 (29 ± 1%). However, the pattern was different when the proteins were loaded together: Hsc70 eluted mainly at volumes 11 (8 ± 1%), 12 (15 ± 1%), 13 (17 ± 1%), 14 (21 ± 1%) and 15 (36 ± 3%) and LmTPR alone elutes mainly at volumes 11 (12 ± 3%), 12 (24 ± 3%), 13 (37 ± 1%) and 14 (26 ± 1%). Summing up, in volumes 11–12 mL, which represent a higher molecular mass than the isolated proteins, the participation of Hsc70 increased from 4 ± 1 to 27 ± 2% and LmTPR from 27 to 36 ± 1%. For raw data see Supplementary Table S3. Additionaly, the mixture fraction was submitted to SEC-MALS that indicated a molecular mass of 130 ± 10 kDA, very similar to the predicted of 136 kDa.

4. Conclusion

A new gene containing a TPR-domain was identified in *Leishmania major* and found to be conserved in other Leishmania species. The translated protein was found to be expressed in all cell cycle stages of the parasite. The TPR-domain was identified by predictors and its structure prediction was characteristic of three tetratricopeptide repeat regions, each arranged in a helix-turn-helix fashion, are packed in a spiral way. To learn more about the protein, the coding DNA was cloned and the recombinant protein, named LmTPR, was purified. The protein was well-folded as shown by its rich alpha-helical structure and by having one tryptophan residue, W144, well buried in the hydrophobic core of the native protein. LmTPR was well stable at the temperatures experienced by the parasite, outside or inside its hosts. The hydrodynamic investigation of LmTPR showed that the protein was a monomer with a nonglobular shape, more likely the parameters indicated a protein with an elongated shape with multiple domains as shown by the

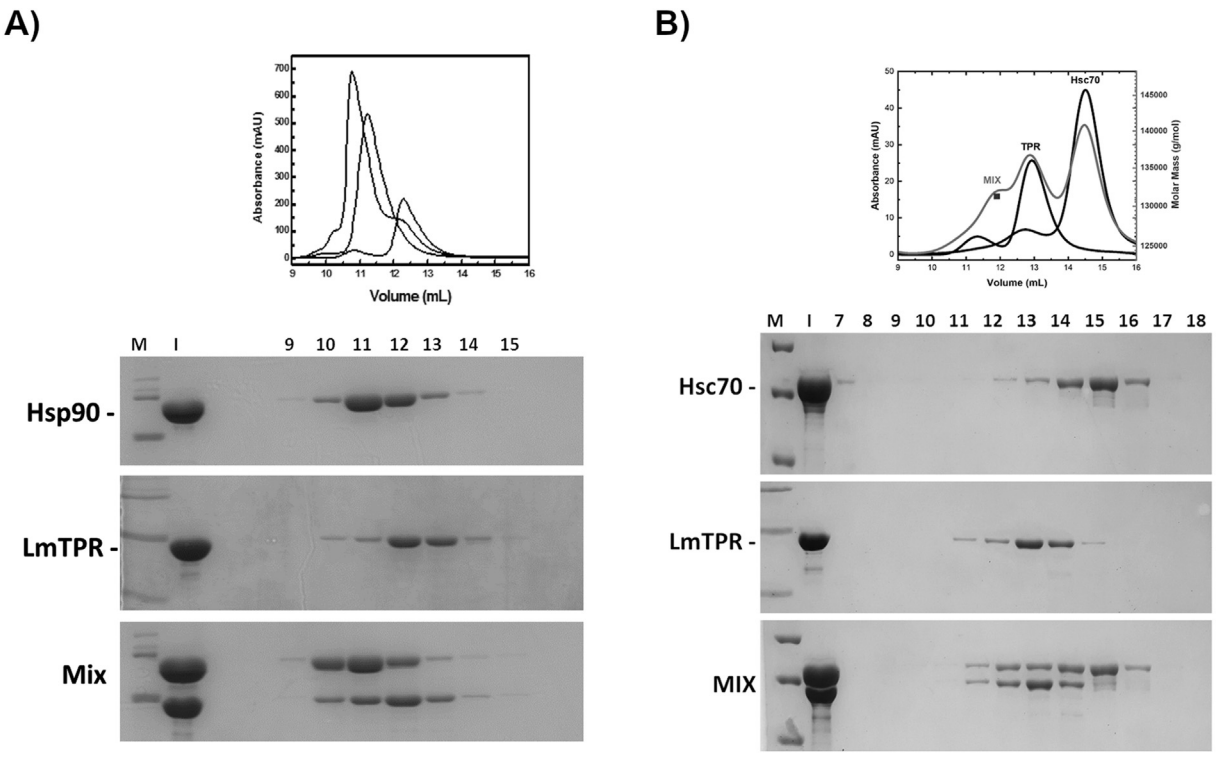

Fig. 6. Interaction with Hsp90 (A) and Hsp70 (B). A) Top) Analytical SEC experiments. LbHsp90 alone, LmTPR protein alone, and a mixture (MIX) of them were loaded (see lane I in the SDS-PAGE at the bottom) and their elution followed by absorbance at 280 nm. Fractions were collected for further SDS-PAGE analysis. The fact that the mixture eluted at a lower volume than the non-mixed proteins indicates a higher molecular mass and therefore interaction. **Bottom)** SDS-PAGE analysis of eluted fractions (9-15) showed in the chromatogram (Top). M, molecular mass standard; I, input. Hsp90 alone eluted mainly in fractions 11 and 12, LmTPR protein alone eluted mainly at fractions 12 and 13, and the mixture containing both proteins at fractions 10 to 12. ImageJ analysis was used to support the interaction between Hsp90 and the LmTPR protein (please, see text for details). As a control, BSA was used as a dummy protein and no interaction was detected (Supplementary Fig. S3A). **B) Top)** Analytical SEC experiments. HsHsc70 alone, LmTPR protein alone, and a mixture (MIX) of them were loaded (see lane I in the SDS-PAGE at the bottom) and their elution followed by absorbance at 280 nm. Fractions were collected for further SDS-PAGE analysis. The fact that the mixture eluted at a lower volume than the non-mixed proteins indicates a higher molecular mass and therefore interaction. **Bottom)** SDS-PAGE analysis of eluted fractions (7-18) showed in the chromatogram (Top). M, molecular mass standard; I, input. Hsc70 alone eluted mainly in fractions 14 and 15, LmTPR protein alone eluted mainly at fractions 13 and 14, and the mixture containing both proteins at fractions 11 to 13. ImageJ analysis was used to support the interaction between Hsc70 and the LmTPR protein (please, see text for details). As a control, BSA was used as a dummy protein and no interaction was detected (Supplementary Fig. S3B).

induced unfolding curve profile. Finally, the ability of LmTPR to bind to a Leishmania Hsp90 was confirmed.

Altogether, the results validated LmTPR as a Hsp90 and Hsp70 interactor that contains a TPR domain. Since there is a class of co-chaperones that have both the TPR and RPAP3 domains and are considered Hsp90 co-chaperones [45], it is interesting to note that sequence analysis predicted an RPAP3 domain at the C-terminus, residues 372 to 458, in LmTPR (Fig. 1A). Although Hsp90 is a cytoplasmic chaperone, a small fraction of Hsp90 (about 3% of the total cellular pool) is present in the nucleus [46]. In humans, RPAP3 (RNA polymerase II-associated protein 3) isoform 1 is 665 residues long, has both domains and cooperates with Hsp90 to assemble RNA polymerase II [47,48], and different from isoform 2, which is 631 residues long, can bind PIH1D1 [49]. It also has an intrinsically disordered region between its TPR domains and C-terminus [45], and it is noteworthy that part of the secondary structure of the LmTPR protein appears to be disordered (see CD results). However, the RPAP3 mechanism of function and interaction with other RNA pol and snRNPs are still under investigation [48]. Another co-chaperone, from both Hsp90 and Hsp70, that has both TPR and RPAP3 domain is DmeI/Spag from *Drosophila melanogaster* which is involved in the stabilization of snoRNP and RNA polymerase II proteins [50]. LmTPR is 29% similar to both HsRPAP3 and DmDmeI/Spag and the higher identity is located at the TPR and RPAP3 domains (Supplementary Fig. S5). Thus, it is possible to indicate LmTPR as belonging to the class of Hsp90 interactors that have both the TPR and RPAP3 domains, but further investigation is needed to confirm that.

Authorship contribution

S.A.A, N.G.Q., A.Z.B.A., E.G.O.M., J.C.B.: Data collection, analysis, and interpretation. G.H.M.: SEC/SDS-PAGE. J.C.B., W.A.H., M.I.N.C., C.H.I.R.: Data analysis and interpretation. C.H.I.R.: designed the work. All authors: drafted and critically reviewed the article.

Declaration of competing interest

The authors declare no competing interests.

Acknowledgements

This work was supported by FAPESP (2012/50161-8; 2017/26131-5; 2018/04375-2), and CAPES (99999.004913/2015-09; Brazil). CHIR, MINC and JCB have a research fellowship from CNPq. SAA received a fellowship from CAPES. GHM has a PIBIC/CNPq fellowship. NGQ (2014/25967-4) and EGOM (2019/11496-3) received fellowship from FAPESP. WAH is supported by a CIHR Project grant (PJT-173491).

Appendix A. Supplementary data

Supplementary data to this article can be found online at https://doi.org/10.1016/j.biochi.2020.12.017.

References

[1] R. Zhao, M. Davey, Y.C. Hsu, P. Kaplanek, A. Tong, A.B. Parsons, N. Krogan, G. Cagney, D. Mai, J. Greenblatt, C. Boone, A. Emili, W.A. Houry, Navigating the chaperone network: an integrative map of physical and genetic interactions mediated by the hsp90 chaperone, Cell 120 (2005) 715–727, https://doi.org/10.1016/j.cell.2004.12.024.

[2] K.A. Krukenberg, T.O. Street, L.A. Lavery, D. Agard, Conformational dynamics of the molecular chaperone Hsp90, Q. Rev. Biophys. 44 (2) (2011) 229–255, https://doi.org/10.1017/s0033583510000314.

[3] V.C.H. da Silva, C.H.I. Ramos, The network interaction of the human cytosolic 90 kDa heat shock protein Hsp90: a target for cancer therapeutics, J. Proteomics 75 (10) (2012) 2790–2802, https://doi.org/10.1016/j.jprot.2011.12.028.

[4] P. Sahasrabudhe, J. Rohrberg, M.M. Biebl, D.A. Rutz, J. Buchner, The plasticity of the Hsp90 Co-chaperone system, Mol. Cell 67 (6) (2017) 947–961.e5, https://doi.org/10.1016/j.molcel.2017.08.004.

[5] G.L. Blatch, M. Lassle, The tetratricopeptide repeat: a structural motif mediating protein-protein interaction, Bioessays 21 (11) (1999) 932–939, https://doi.org/10.1002/(sici)1521-1878(199911)21:11<932::aid-bies5>3.0.co;2-n.

[6] L.D. D'Andrea, L. Regan, TPR proteins: the versatile helix, Trends Biochem. Sci. 28 (12) (2003) 655–662, https://doi.org/10.1016/j.tibs.2003.10.007.

[7] C. Scheufler, A. Brinker, G. Bourenkov, S. Pegoraro, L. Moroder, H. Bartunik, F.U. Hartl, I. Moarefi, Structure of TPR domain–peptide complexes: critical elements in the assembly of the Hsp70–Hsp90 multichaperone machine, Cell 101 (2) (2000) 199–210, https://doi.org/10.1016/S0092-8674(00)80830-2.

[8] WHO. World Health Organization, Global leishmaniasis update, 2006-2015: a turning point in leishmaniasis surveillance, Wkly. Epidemiol. Rec. 92 (2017) 557–572.

[9] D.T. Jones, Protein secondary structure prediction based on position-specific scoring matrices, J. Mol. Biol. 292 (1999) 195–202.

[10] A. Drozdetskiy, C. Christian, J. Procter, G.J. Barton, JPred4: a protein secondary structure prediction server, Nucleic Acids Res. 43 (W1) (2015) W389–W394, https://doi.org/10.1093/nar/gkv332.

[11] S. Hunter, R. Apweiler, T.K. Attwood, A. Bairoch, A. Bateman, D. Binns, P. Bork, U. Das, L. Daugherty, L. Duquenne, R.D. Finn, J. Gough, D. Haft, N. Hulo, D. Kahn, E. Kelly, A. Laugraud, I. Letunic, D. Lonsdale, R. Lopez, M. Madera, J. Maslen, C. McAnulla, J. McDowall, J. Mistry, A. Mitchell, N. Mulder, D. Natale, C. Orengo, A.F. Quinn, J.D. Selengut, C.J.A. Sigrist, M. Thimma, P.D. Thomas, F. Valentin, D. Wilson, C.H. Wu, C. Yeats, InterPro: the integrative protein signature database, Nucleic Acids Res. 37 (1) (2009) D211–D215, https://doi.org/10.1093/nar/gkn785.

[12] S. El-Gebali, J. Mistry, A. Bateman, S.E. Reddy, A. Luciany, S.C. Potter, M. Quereshi, L.J. Richardson, G.A. Salazar, A. Smart, E.L.L. Sonnhammer, L. Hirsh, L. Paladin, D. Piovesan, S.C.E. Tosatto, R.D. Finn, The Pfam protein families database in 2019, Nucleic Acids Res. 47 (D1) (2019) D427–D432, https://doi.org/10.1093/nar/gky995.

[13] C.J.A. Sigrist, E. de Castro, L. Cerutti, B.A. Cuche, N. Hulo, A.J. Bridge, L. Bougueleret, I. Xenarios, New and continuing developments at PROSITE, Nucleic Acids Res. 41 (2012), https://doi.org/10.1093/nar/gks1067.

[14] F. Sievers, A. Wilm, D. Dineen, T.J. Gibson, K. Karplus, W. Li, R. Lopez, H. McWilliam, M. Remmert, J. Söding, J.D. Thompson, D.G. Higgins, Fast, scalable generation of high-quality protein multiple sequence alignments using Clustal Omega, Mol. Syst. Biol. 7 (2011) 539, https://doi.org/10.1038/msb.2011.75.

[15] S.F. Altschul, W. Gish, W. Miller, E.W. Myers, D.J. Lipman, Basic local alignment search tool, J. Mol. Biol. 215 (1990) 403–410, https://doi.org/10.1016/S0022-2836(05)80360-2.

[16] D. Xu, Y. Zhang, Ab initio protein structure assembly using continuous structure fragments and optimized knowledge-based force field, Proteins 80 (2012) 1715–1735, https://doi.org/10.1002/prot.24065.

[17] D. Xu, Y. Zhang, Toward optimal fragment generations for ab initio protein structure assembly, Proteins 81 (2013) 229–239, https://doi.org/10.1002/prot.24179.

[18] C.T. Rueden, J. Schindelin, M.C. Hiner, B.E. DeZonia, A.E. Walter, E.T. Arena, K.W. Eliceiri, ImageJ2: ImageJ for the next generation of scientific image data, BMC Bioinf. 18 (2017) 529, https://doi.org/10.1186/s12859-017-1934-z.

[19] H. Edelhoch, Spectroscopic determination of tryptophan and tyrosine in proteins, Biochemistry 6 (1967) 1948–1954.

[20] K.P. Silva, T.V. Seraphim, J.C. Borges, Structural and functional studies of Leishmaia braziliensis Hsp90, Biochim. Biophys. Acta 1834 (2013) 351–361, https://doi.org/10.1016/j.bbapap.2012.08.004.

[21] J.C. Borges, C.H.I. Ramos, Characterization of nucleotide-induced changes on the structure of human 70 kDa heat shock protein Hsp70.1 by analytical ultracentrifugation, BMB Rep. 42 (2009) 166–171.

[22] C.L. Barbiéri, A.I. Doine, E. Freymuller, Lysosomal depletion in macrophages from spleen and foot lesions of Leishmania-infected hamster, Exp. Parasitol. 71 (2) (1990) 218–228, https://doi.org/10.1016/0014-4894(90)90024-7.

[23] R. da Silva, D.L. Sacks, Metacyclogenesis is a major determinant of Leishmania promastigote virulence and attenuation, Infect. Immun. 55 (1987) 2802–2806.

[24] B. Cuypers, M.A. Domagalska, P. Meysman, G. de Muylder, M. Vanaerschot, H. Imamura, F. Dumetz, T.W. Verdonckt, P.J. Myler, G. Ramasamy, K. Laukens, J.-C. Dujardin, Multiplexed spliced-708 leader sequencing: a high-throughput, selective method for RNA-seq in trypanosomatids, Sci. Rep. 7 (2017) 3725, https://doi.org/10.1038/s41598-017-03987-0.

[25] B. Langmead, S.L. Salzberg, Fast gapped-read alignment with Bowtie 2, Nat. Methods 9 (2012) 357–359, https://doi.org/10.1038/nmeth.1923.

[26] T. Carver, S.R. Harris, M. Berriman, J. Parkhill, J.A. McQuillan, Artemis: an integrated platform for visualization and analysis of high-throughput sequence-based experimental data, Bioinformatics 28 (4) (2012) 464–469, https://doi.org/10.1093/bioinformatics/btr703.

[27] A. Mortazavi, B.A. Williams, K. McCue, L. Schaeffer, B. Wold, Mapping and quantifying mammalian transcriptomes by RNA-Seq, Nat. Methods 5 (2008) 621–628, https://doi.org/10.1038/nmeth.1226.

[28] D. Correa, C.H.I. Ramos, The use of circular dichroism spectroscopy to study protein folding, form and function, Afr. J. Biochem. Res. 3 (2009) 164–173.

[29] J.C. Borges, C.H.I. Ramos, Analysis of molecular targets of Mycobacterium tuberculosis by analytical ultracentrifugation, Curr. Med. Chem. 18 (2011) 1276–1285, https://doi.org/10.2174/092986711795029537.

[30] S.M.R. Teixeira, B.M. Valente, Mechanisms controlling gene expression in trypanosomatids, Front. Parasitol. 1 (2017) 261–290.

[31] K.K. Mishra, T.R. Holzer, L.L. Moore, J.H. LeBowitz, A Negative Regulatory Element Controls mRNA Abundance of the *Leishmania Mexicana* Paraflagellar Rod Gene *PFR2* Eukaryotic Cell, vol. 2, 2003, pp. 1009–1017, https://doi.org/10.1128/EC.2.5.1009-1017.2003.

[32] A. Rochette, F. McNicoll, J. Girard, M. Breton, E. Leblancc, M.G. Bergeron, B. Papadopoulou, Characterization and developmental gene regulation of a large gene family encoding amastin surface proteins in Leishmania spp, Mol. Biochem. Parasitol. 140 (2005) 205–220, https://doi.org/10.1016/j.molbiopara.2005.01.006.

[33] E.J.R. Vasconcelos, M.C. Terrão, J.C. Ruiz, R.Z.N. Vêncio, A.K. Cruz, In silico identification of conserved intercoding sequences in Leishmania genomes: unraveling putative cis-regulatory elements, Mol. Biochem. Parasitol. 183 (2012) 140–150, https://doi.org/10.1016/j.molbiopara.2012.02.009.

[34] E. Inbar, V.K. Hughitt, L.A.L. Dillon, K. Ghosh, N.M. El-Sayed, D.L. Sacks, The transcriptome of *Leishmania major* developmental stages in their natural sand fly vector, mBio 8 (2017), e00029-17, https://doi.org/10.1128/mBio.00029-17.

[35] N.S. Akopyants, R.S. Matlib, E.N. Bukanova, M.R. Smeds, B.H. Brownstein, G.D. Stormo, S.M. Beverley, Expression profiling using random genomic DNA microarrays identifies differentially expressed genes associated with three major developmental stages of the protozoan parasite Leishmania major, Mol. Biochem. Parasitol. 136 (2004) 71–86, https://doi.org/10.1016/j.molbiopara.2004.03.002.

[36] A. Saxena, T. Lahav, N. Holland, G. Aggarwal, A. Anupama, Y. Huang, H. Volpin, P.J. Myler, D. Zilberstein, Analysis of the Leishmania donovani transcriptome reveals an ordered progression of transient and permanent changes in gene expression during differentiation, Mol. Biochem. Parasitol. 152 (2007) 53–65, https://doi.org/10.1016/j.molbiopara.2006.11.011.

[37] S. Haile, B. Papadopoulou, Developmental regulation of gene expression in trypanosomatid parasitic protozoa, Curr. Opin. Microbiol. 10 (2007) 569–577, https://doi.org/10.1016/j.mib.2007.10.001.

[38] P.J. Alcolea, A. Alonso, R. Molina, M. Jiménez, P.J. Myler, V. Larraga, Functional genomics in sand fly–derived *Leishmania* promastigotes, PLoS Neglected Trop. Dis. 13 (2019), e0007288, https://doi.org/10.1371/journal.pntd.0007288.

[39] C.A. Royer, Probing protein folding and conformational transitions with fluorescence, Chem. Rev. 106 (5) (2006) 1769–1784.

[40] S.M. Gossage, M.E. Rogers, P.A. Bates, Two separate growth phases during the development of Leishmania in sand flies: implications for understanding the life cycle, Int. J. Parasitol. 33 (10) (2003) 1027–1034, https://doi.org/10.1016/S0020-7519(03)00142-5.

[41] R. Back, C. Dominguez, B. Rothé, C. Bobo, C. Beaufils, Solange Moréra, P. Meyer, B. Charpentier, C. Branlant, F.H.- T Allain, X. Manival, High-resolution structural analysis shows how Tah1 tethers Hsp90 to the R2TP complex, Structure 21 (10) (2013) 1834–1847, https://doi.org/10.1016/j.str.2013.07.024.

[42] F.A.H. Batista, T.V. Seraphim, C.A. Santos, M.R. Gonzaga, L.R.S. Barbosa, C.H.I. Ramos, J.C. Borges, Low sequence identity but high structural and functional conservation: the case of Hsp70/Hsp90 organizing protein (Hop/Sti1) of Leishmania braziliensis, Arch. Biochem. Biophys. 600 (2016) 12–22, https://doi.org/10.1016/j.abb.2016.04.008.

[43] C.C. Gonçalves Cc, G.M.S. Pinheiro, K.M. Dahlström, D.E.P. Souto, L.T. Kubota, L.R.S. Barbosa, C.H.I. Ramos, On the structure and function of Sorghum bicolor CHIP (carboxyl terminus of Hsc70-interacting protein): a link between chaperone and proteasome systems, Plant Sci. 296 (2020), https://doi.org/10.1016/j.plantsci.2020.110506.

[44] A.L.S. Coto, T.V. Seraphim, F.A.H. Batista, P.R. Dores-Silva, A.B.F. Barranco, F.R. Teixeira, L.M. Gava, J.C. Borges, Structural and functional studies of the Leishmania braziliensis SGT co-chaperone indicate that it shares structural features with HIP and can interact with both Hsp90 and Hsp70 with similar affinities, Int. J. Biol. Macromol. 118 (2018) 693–706, https://doi.org/10.1016/j.ijbiomac.2018.06.123.

[45] J. Henri, M.E. Chagot, M. Bourguet, Y. Abel, G. Terral, C. Maurizy, C. Aigueperse, F. Georgescauld, F. Vandermoere, R. Saint-Fort, I. Behm-Ansmant,

B. Charpentier, B. Pradet-Balade, C. Verheggen, E. Bertrand, P. Meyer, S. Cieanférani, X. Manival, M. Quinternet, Deep structural analysis of RPAP3 and PIH1D1, two components of the HSP90 Co-chaperone R2TP complex, Structure 26 (9) (2018) 1196–1209e8, https://doi.org/10.1016/j.str.2018.06.002.

[46] G.A. Berbers, R. Kunnen, P.M. van Bergen en Henegouwen, R. van Wijk, Localization and quantitation of hsp84 in mammalian cells, Exp. Cell Res. 177 (1988) 257–271, https://doi.org/10.1016/0014-4827(88)90460-0.

[47] S. Boulon, B. Pradet-Balade, C. Verheggen, D. Molle, S. Boireau, M. Georgieva, K. Azzag, M.-C. Robert, Y. Ahmad, H. Neel, A.I. Lamond, E. Bertrand, HSP90 and its R2TP/Prefoldin-like cochaperone are involved in the cytoplasmic assembly of RNA polymerase II, Mol. Cell 39 (6) (2010) 912–924, https://doi.org/10.1016/j.molcel.2010.08.023.

[48] F. Martino, M. Pal, H. Muñoz-Hernández, C.F. Rodríguez, R. Núnes-Ramíres, D. Gil-Carton, G. Degliesposti, J.M. Skehel, S.M. Roe, C. Prodromou, L.H. Pearl, O. Llorca, RPAP3 provides a flexible scaffold for coupling HSP90 to the human R2TP co-chaperone complex, Nat. Commun. 9 (2018) 1501, https://doi.org/10.1038/s41467-018-03942-1.

[49] M. Yoshida, M. Saeki, H. Egusa, Y. Irie, Y. Kamano, S. Uraguchi, M. Sotozono, H. Niwa, Y. Kamisaki, RPAP3 splicing variant isoform 1 interacts with PIH1D1 to compose R2TP complex for cell survival, Biochem. Biophys. Res. Commun. 430 (2013) 320–324, https://doi.org/10.1016/j.bbrc.2012.11.017.

[50] N.E.H. Benbahouche, I. Iliopoulos, I. Török, J. Marhold, J. Henri, A.V. Kajava, R. Farkaš, T. Kempf, M. Schnölzer, P. Meyer, I. Kiss, E. Bertrand, B.M. Mechler, B. Pradet-Balade, Drosophila Spag is the homolog of RNA polymerase II-associated protein 3 (RPAP3) and recruits the heat shock proteins 70 and 90 (Hsp70 and Hsp90) during the assembly of cellular machineries, J. Biol. Chem. 289 (9) (2014) 6236–6247, https://doi.org/10.1074/jbc.M113.499608.